High-intensity focused ultrasound beam path visualization using ultrasound imaging

초음파 영상을 이용한 고강도 집중 초음파 빔 시각화

Jae Hee Song,[1] Jin Ho Chang,[2] and Yang Mo Yoo[2] [†]

(송재희,[1] 장진호,[2] 유양모[2†])

[1]Queenland Brain Institute, University of Queenland
[2]Departments of Electronic Engineering and Biomedical Engineering, Sogang University
(Received May 14, 2019; accepted January 10, 2020)

ABSTRACT: In High-Intensity Focused Ultrasound (HIFU) treatment, effective localization of HIFU focus is important for developing a safe treatment plan. While Magnetic Resonance Imaging guided HIFU (MRIgHIFU) can visualize the ultrasound path during the treatment for localizing HIFU focus, it is challenging in ultrasound imaging guided HIFU (USIgHIFU). In the present study, a real-time ultrasound beam visualization technique capable of localizing HIFU focus is presented for USIgHIFU. In the proposed method, a short pulse, with the same center frequency of an imaging ultrasound transducer below the regulated acoustic intensity (i.e., Ispta < 720 mW/cm^2), was transmitted through a HIFU transducer whereupon backscattered signals were received by the imaging transducer. To visualize the HIFU beam path, the backscattered signals underwent dynamic receive focusing and subsequent echo processing. From in vitro experiments with bovine serum albumin gel phantoms, the HIFU beam path was clearly depicted with low acoustic intensity (i.e., Ispta of 94.8 mW/cm^2) and the HIFU focus was successfully localized before any damages were produced. This result indicates that the proposed ultrasound beam path visualization method can be used for localizing the HIFU focus in real time while minimizing unwanted tissue damage in USIgHIFU treatment.

Keywords: High-intensity focused ultrasound, Ultrasound image guidance, Focal point position, Ultrasound beam path

PACS numbers: 43.35.Wa, 43.35.Yb

초   록: 고강도 집중 초음파(High-Intensity Focused Ultrasound, HIFU) 치료에서 HIFU 초점의 효과적인 위치 파악은 안전한 치료 계획을 개발하는 데 중요하다. 자기 공명 영상 유도 HIFU(Magnetic Resonance Imaging guided HIFU, MRIgHIFU)는 HIFU 초점을 영상화하여 치료 중에 초음파 경로를 시각화 할 수 있지만 초음파 이미징 유도 HIFU (Ultrasound imaging guided HIFU, USIgHIFU)에서는 어려움이 있다. 본 연구에서는 USIgHIFU에 대해 HIFU 초점을 영상화할 수 있는 실시간 초음파 빔 시각화 기법을 제시 하였다. 제안 된 방법에서, 음향 강도(Ispta < 720 mW/cm^2) 아래의 이미징 초음파 변환자의 동일한 중심 주파수를 갖는 짧은 펄스가 HIFU 변환기를 통해 전송되고, HIFU 빔 경로를 시각화하기 위해 수신 신호는 동적 수신 포커싱 및 후속 에코 처리를 거쳤다. 소 혈청 알부민 젤 팬텀을 이용한 생체 외 실험으로부터, HIFU 빔 경로는 낮은 음향 강도 (Ispta = 94.8 mW/cm^2)에서도 명확히 영상화 할 수 있었고 HIFU 초점은 손상이 생성되기 전에 성공적으로 시각화하였다. 이 결과는 제안 된 초음파 빔 경로 시각화 방법이 USIgHIFU 치료에서 원치 않는 조직 손상을 최소화하면서 실시간으로 HIFU 초점을 영상화하는 데 사용될 수 있음을 나타낸다.

핵심용어: 고강도 집중 초음파, 초음파 이미징 유도 치료, 초점 위치 파악, 초음파 빔 경로

†**Corresponding author:** Yangmo Yoo (ymyoo@sogang.ac.kr)
Department of Electronic Engineering and Biomedical Engineering, Sogang University, 35 Baekbeom-ro, Mapo-gu 04107, Republic of Korea
(Tel: 82-2-705-4731, Fax: 82-2-707-3008)

I. Introduction

High-Intensity Focused Ultrasound (HIFU) has received increasing interest as a thermal ablation tumor therapy due

to its noninvasive and accurate targeting ability.[1-3] In HIFU treatment, by focusing acoustic energy on specific areas where temperature rises and cavitation is generated, only an abnormal tissue could be locally treated without damaging surrounding healthy tissues.[4-6] From previous studies, HIFU treatment has shown promising therapeutic effects in different types of tumors, such as uterine leiomyomas, liver tumors, thyroid tumors, renal cell carcinoma, bone metastasis, pancreatic cancers and breast cancers.[7-17]

In HIFU treatment, as temperature at the HIFU focal site rises higher than 60°C within a few seconds and inertia cavitation generates irregular lesions, effective pre-targeting and monitoring in real time is essential for the patient's safety.[6,18-19] Currently, Magnetic Resonance Imaging and ultrasound imaging (i.e., MRIgHIFU and USIgHIFU) are utilized as a guidance and monitoring modality. MRI can localize HIFU focus since it can visualize the ultrasound beam path.[20] In addition, it can show temperature evaluation during HIFU treatment.[21] However, it is difficult to achieve real-time monitoring due to a long image acquisition time.[6,22] On the other hand, USI has the potential to provide real-time guidance of HIFU treatment at a relatively low cost.[23]

Several groups have investigated targeting and monitoring techniques based on USI. The changes of physical properties (e.g., speed of sound, attenuation coefficient and elastic modulus) of targeted tissues during HIFU treatment have been assessed to localize HIFU lesions.[24-28] Advantages and disadvantages of each technique were comprehensively summarized elsewhere.[6] Among various USIgHIFU methods, acoustic backscattering and interference-based methods were proposed as a pre-targeting technique to localize HIFU focus with low acoustic intensity.[6,18] However, unlike MRIgHIFU, there is currently no method to visualize the HIFU beam path for USIgHIFU. The HIFU beam path visualization is important for avoiding any adverse damages in surrounding tissues during HIFU treatment since it can not only localize HIFU focus, but also predict any potential risks

from unwanted localized heating by means of refraction and attenuation.[29-30] Therefore, real-time HIFU beam path visualization is essential for enhancing the efficacy of HIFU treatment, providing more accurate and robust surgical planning.

In this paper, a precise and safe HIFU beam path and focus visualization method based on an ultrasound B-mode imaging is presented. Backscattered signals after HIFU exposure were directly used for generating a HIFU targeting image, in which the HIFU beam path and focus were determined, using coherent beamforming and subsequent echo processing. The proposed method was evaluated with Bovine Serum Albumin (BSA) gel phantoms using a custom-built HIFU treatment system.

II. Materials and Methods

2.1 Experimental set-up

The overall block diagram of the experimental set-up is shown in Fig. 1(a). A single element broad bandwidth
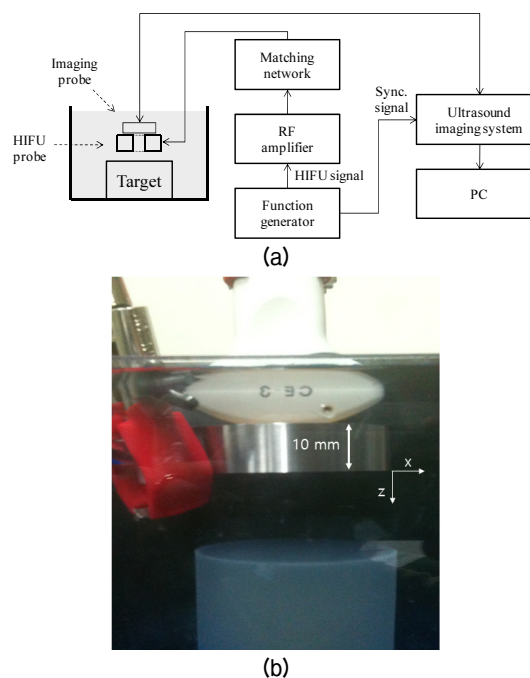

(a)

(b)

Fig. 1. (Color online) (a) In vitro experimental setup for the pre-targeting and treatment of HIFU and the (b) setup for HIFU and imaging probes in the in vitro experiment.

HIFU transducer (H-102, Sonic Concepts, Bothell, WA, USA) was used in this experiment. It operated at 1.1 MHz and accommodated a 20 mm central opening for imaging. The geometric focal depth of the HIFU transducer was 62.6 mm. A function generator (AFG3252, Tektronix Inc., Beaverton, OR, USA) generated the HIFU driving signal for targeting and lesion formation. As shown in Fig. 1(a), this signal was amplified by a radio-frequency (RF) power amplifier (75A250A, Amplifier Research Corp., Souderton, PA, USA) and transmitted to a target in the water tank through the supplied RF impedance matching network, resonating at the fundamental resonance near 1.1 MHz. The water tank contained degassed water, which was prepared by boiling tap water and subsequently cooling it to room temperature.[18] A commercial research ultrasound imaging system platform (SonixTOUCH, Ultrasonix Medical Corp., Richmond, BC, Canada) synchronized at each HIFU exposure was used for acquiring received backscattered HIFU signals from BSA gel phantoms containing agar particles as scatterers.[31] The weight/ volume (w/v) concentrations of BSA and agar particles were 5 % and 0.4 %, respectively. A curved linear C5-2 probe was used for receiving backscattered signals, operating at a center frequency of 3.3 MHz and a frequency bandwidth of 2 MHz to 5 MHz. The setup for HIFU and imaging probes is shown in Fig. 1(b). All post-beamformed RF data were recorded in the internal memory of the SonixTOUCH research platform and then transferred to a PC for further processing to generate a HIFU beam path image.

2.2 Acoustic intensity measurement

Acoustic intensity during pre-targeting was measured for validating the safety of the proposed method. An Acoustic Intensity Measurement System (AIMS, Onda Corporation, Sunnyvale, CA, USA) with 6 axes and a capsule hydrophone (HGL-0200, Onda Corporation, Sunnyvale, CA, USA) were used for the measurement. The HIFU transducer and the hydrophone were aligned manually because the AIMS software did not work for the

H-102 HIFU transducer due to its double peak outside the focal depth.

After the alignment, the hydrophone was moved laterally from -10 mm to 10 mm and axially from 40 mm to 90 mm with 0.5 mm spacing, respectively. At each position, pre-targeting signals were transmitted and then received by the hydrophone. By repeating this process five times, temporal average intensity was measured on a XZ plane from which spatial peak temporal average intensity (I_{spta}) was derived.

2.3 HIFU beam path visualization

Pre-targeting and HIFU treatment experiments were conducted sequentially. After the HIFU focus was predicted with low acoustic intensity from a beam path image, a HIFU lesion was generated by increasing the HIFU output. To evaluate the performance of the proposed pre-targeting method, the location of the predicted HIFU focus was compared with a lesion from HIFU treatment. Due to the different purposes of pre-targeting and therapy experiments, as listed in Table 1, different experiment parameters were used.

Before pre-targeting, a reference ultrasound image of target areas was obtained without HIFU exposure. In the pre-targeting phase, the acoustic intensity of transmitted HIFU signals was decreased sufficiently so as to not damage targeting areas. The center frequency of the HIFU probe was set to be the same as that of an imaging probe (i.e., 3.3 MHz) and the pulse duration was set to 1.5 s (i.e., 5 cycles) for preserving spatial resolution. The pulse excitation of the SonixTOUCH platform was turned off (i.e., the imaging probe was turned off) and each HIFU

Table 1. Parameters used in the in vitro experiment.

	Pre-targeting phase	Treatment phase
Acoustic intensity (I_{spta})	94.8 mW/cm²	-
Center frequency	3.3 MHz	1.1 MHz
Pulse length	5 cycles	176,000 cycles
Time delay from trigger	0	13 ms
Pulse repetition frequency	-	5 Hz

exposure was synchronized with the scanline onset timing. All backscattered signals were beamformed and written to the internal memory of the SonixTOUCH platform. Then, beamformed signals were processed with a custom echo processing module running on MATLAB (Mathworks Inc., Natick, MA, USA). After echo processing, the HIFU beam path image was generated and the HIFU focus was identified as the crossing area in the HIFU beam path.

In the HIFU treatment phase, HIFU exposure conditions were changed as listed in Table 1. The output power of a HIFU probe was increased with the pulse repetition frequency at 5 Hz and the duty cycle at 80 %. The excitation frequency was set to 1.1 MHz, which was the resonance frequency of the HIFU probe. Since it was difficult to measure the acoustic intensity of the HIFU output for the treatment phase, the amplitude of the driving signal and the gain of the RF power amplifier were determined empirically. To monitor a lesion formation process with minimal HIFU interference, the modified HIFU real-time visualization method with time sharing was applied.[8] In this time sharing HIFU monitoring method, HIFU excitation was synchronized with the imaging frame onset and delayed by 13 ms to localize the HIFU interference area out of the Region Of Interest (ROI). The HIFU lesion was formed with a HIFU exposure time of approximately 120 s and an ultrasound image including the formed lesion was captured. Finally, the lesion location was compared with the predicted one in order to verify the accuracy of the proposed method.

III. Results and Discussion

As shown in Fig. 2, the BSA gel phantom was placed about 45 mm away from the US transducer and showed homogeneous backscattering. Parallel lines between 30 mm and 40 mm were considered reverberation patterns. Due to the HIFU transducer's small opening for imaging, interference patterns were formed at the left and right side of the phantom. The Dynamic Range (DR) was set to 80 dB.

Fig. 2. Ultrasound image of the BSA phantom before HIFU exposure.
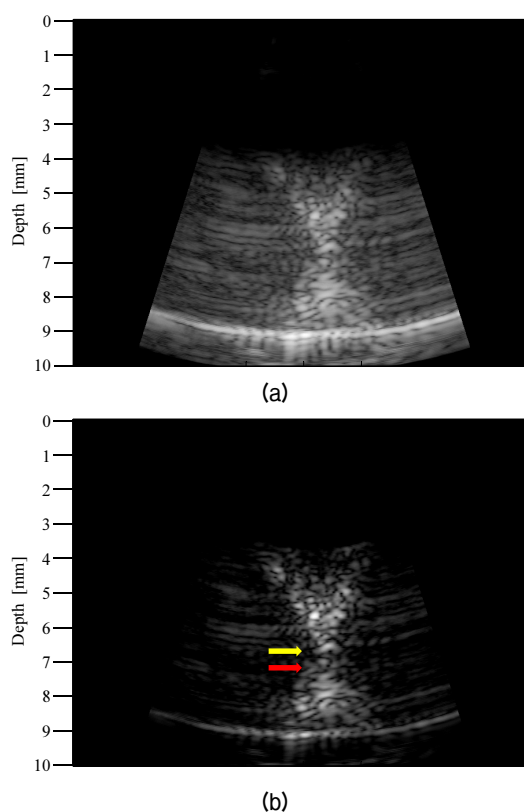

(a)

(b)

Fig. 3. (Color online) HIFU beam path image (a) before and (b) after controlling imaging parameters, using low intensity HIFU emission (i.e., derated Ispta = 94.8 mW/cm^2) during the pre−targeting phase.

Fig. 3(a) shows the obtained HIFU beam path image before the optimization of the imaging parameters, such that the HIFU beam path is not clearly depicted.

To enhance the HIFU beam path, the Time Gain Compensation (TGC), gain and DR were properly set, as shown in Fig. 3(b).
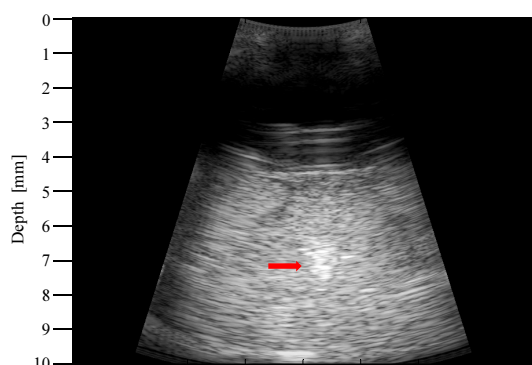
Fig. 4. (Color online) Ultrasound image of the BSA phantom after HIFU lesion formation.

Fig. 5. (Color online) Photograph of BSA phantom containing HIFU-induced lesion: (a) top view, (b) side view and (c) cross-sectional view.

The TGC was controlled to show homogeneous echogenicity in the HIFU beam path image and the gain value was lowered in order to suppress background noise. Similarly, the DR value was changed from 80 dB to 45 dB to make the beam path distinct from the background. As shown in Fig. 3(b), the shape of the beam path appeared as an '×' because acoustic energy could not be emitted from the central area of the HIFU transducer due to its opening for imaging. During the pre-targeting phase, HIFU lesions, which can be easily recognized in the transparent BSA gel phantom, did not form.

The crossing point of the beam path (at 67 mm), indicated by a yellow arrow in Fig. 3(b), can be considered as the HIFU focus since maximum scattering occurs at the focus of the HIFU transducer.

Fig. 4 shows the ultrasound image of the BSA phantom after the HIFU lesion formation. The image was produced by transmitting a short excitation pulse via an imaging probe. As indicated by the red arrow in Fig. 4, the center of the HIFU lesion was located around 72 mm. The yellow and red arrows were plotted together in Fig. 3(b) to compare the predicted HIFU lesion to the actual one. As shown in Fig. 3(b), the distance between the predicted and actual HIFU lesions was 5 mm. This difference occurred because of the gap [10 mm as shown in Fig. 1(b)] between the HIFU and imaging probe. During the pre-targeting phase, the HIFU signal traveled 10 mm less than the imaging signal such that the predicted lesion, as shown in Fig. 3(b), was actually 5 mm closer to the imaging probe
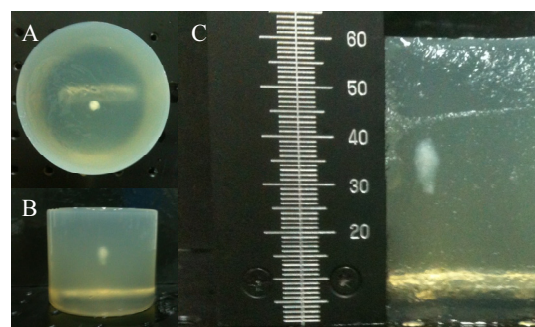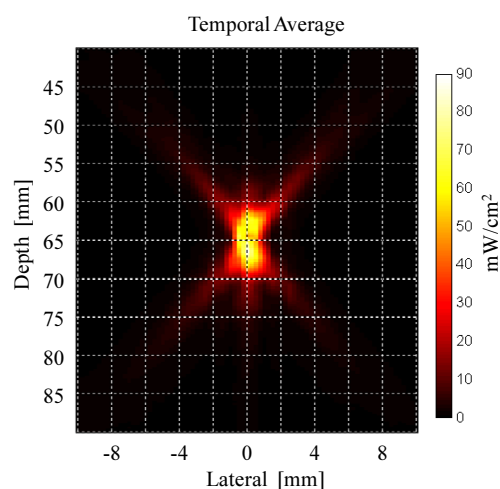

Fig. 6. (Color online) A measured HIFU beam profile.

when considering a round trip time. The formed HIFU lesion was easily recognizable in the BSA gel phantom, as shown in the photographs of Fig. 5.

For further assessment, the cross-sectional view of the BSA gel phantom is shown in Fig. 5(c). The HIFU lesion formed at approximately 25 mm below the surface of the BSA gel phantom, which was located at around 45 mm from the surface of the HIFU probe. Therefore, HIFU lesion was at approximately 70 mm from the HIFU probe, close to the estimated location of 72 mm. The difference of 2 mm occurred because the location was measured based on the center of the lesion while HIFU lesions were growing toward the HIFU probe.[32] Fig. 6 shows a measured HIFU beam profile during the pre-targeting phase. The beam profile is similar to the HIFU beam path shown in Fig. 3. The focal depth from the measurement

was 65.0 mm compared to the 62.6 mm from the data sheet. The discrepancy of 2.4 mm can be attributed to measurement errors. From the HIFU beam profile, the derated Ispta, was measured as 94.8 mW/cm^2 while the regulated value by the Food and Drug Administration is 720 mW/cm^2.

The HIFU beam path visualization technique using an ultrasound B-mode imaging with low acoustic intensity was proposed.

For pre-targeting, a short pulse with a center frequency of 3.3 MHz was excited via a HIFU probe while turning off the emission from an ultrasound imaging probe. Consequently, backscattered signals were received using the imaging probe. When a 1.1 MHz center frequency pulse is used as a HIFU excitation signal, the 3rd harmonic component of received signals, which is matched to the center frequency of the imaging probe, can be used for pre-targeting. However, to generate the 3rd harmonic signal, an increased acoustic intensity is required. Thus, it is necessary for HIFU pre-targeting to use an elevated frequency pulse (e.g., 3.3 MHz) when safety is concerned. Although the HIFU beam path can be successfully visualized on a B-mode ultrasound image, further investigations are required for confirming its accuracy and robustness. All pre-beamformed RF signals should be captured and then received beamforming needs to account for the gap between the HIFU and imaging probes. It must be noted that no study has shown a HIFU-induced beam path with low acoustic intensity using an ultrasound imaging system.

The HIFU treatment can be more safely guided with beam path information than when only guided with focus location. For example, the effect of acoustic obstacles, such as bones, can be easily recognized in a HIFU beam path image even though they are not shown on normal ultrasound imaging due to the different geometries of HIFU and imaging probes. When treating targets near bones, the HIFU treatment process should be guided carefully due to a bone's higher absorption when compared to normal tissues. With the known HIFU beam path and

tissue absorption coefficients, the relative energy deposition ratio between the target and the obstacles (e.g., bone) can be estimated. If a HIFU array probe is available, the quality of HIFU focus can be estimated with low acoustic intensity and optimized by varying the transmit delays. Therefore, the real-time feedback from the beam path visualization can considerably enhance the efficacy of the HIFU treatment by optimizing its sonification parameters.

IV. Conclusions

In this paper, a HIFU beam path visualization method using conventional ultrasound B-mode imaging has been presented. From in vitro experiments, the proposed beam visualization method successfully localized the HIFU focus with low acoustic intensity and it was confirmed with the visual assessment of the formed HIFU lesion. This result indicates that the proposed HIFU beam path visualization method can enhance the efficacy of the ultrasound guided HIFU treatment while preventing adverse effects. Further validation with in vitro experiments concerning tissue samples and with in vivo experiments is required for clinical uses.

References

1. G. ter Haar, "Therapeutic ultrasound," Eur. J. Ultrasound, **9**, 3-9 (1999).
2. G. ter Haar, "High intensity ultrasound," Surg. Innov. **8**, 77-89 (2001).
3. J. E. Kennedy, "High-intensity focused ultrasound in the treatment of solid tumours," Nat. Rev. Cancer, **5**, 321-327 (2005).
4. D. Arora, D. Cooley, T. Perry, M. Skliar, and R. B. Roemer, "Direct thermal dose control of constrained focused ultrasound treatments: phantom and in vivo evaluation," Phys. Med. Biol. **50**, 1919-1935 (2005).
5. J. Seo, B. C. Tran, T. L. Hall, J. B. Fowlkes, G. B. Abrams, M. O'Donnell, and C. A. Cain, "Evaluation of ultrasound tissue damage based on changes in image echogenicity in canine kidney," IEEE Trans. Ultrason. Ferroelect. Freq. Contr. **52**, 1111-1120 (2005).
6. S. Vaezy, X. Shi, R. W. Martin, E. Chi, P. I. Nelson, M. R. Bailey, and L. A. Crum, "Real-time visualization

of high-intensity focused ultrasound treatment using ultrasound imaging," Ultrasound Med. Biol. **27**, 33-42 (2001).

7. R. Catane, A. Beck, Y. Inbar, T. Rabin, N. Shabshin, S. Hengst, R. M. Pfeffer, A. Hanannel, O. Dogadkin, B. Liberman, and D. Kopelman, "MR-guided focused ultrasound surgery (MRgFUS) for the palliation of pain in patients with bone metastases - preliminary clinical experience," Ann. Oncol. **18**, 163-167 (2007).

8. O. Esnault, B. Franc, J. P. Monteil, and J. Y. Chapelon, "High-intensity focused ultrasound for localized thyroid-tissue ablation: Preliminary experimental animal study," Thyroid, **14**, 102-1076 (2004).

9. H. Furusawa, K. Namba, H. Nakahara, C. Tanaka, Y. Yasuda, E. Hirabara, M. Imahariyama, and K. Komaki, "The evolving non-surgical ablation of breast cancer: MR guided focused ultrasound (MRgFUS)," Breast Cancer, **14**, 55-58 (2007).

10. J. H. Hwang and L. A. Crum, "Current status of clinical high-intensity focused ultrasound," Proc. the 31st Annual International Conference of the IEEE EMBS. Minnea-polis, MN, USA, 130-133 (2008).

11. J. E. Kennedy and G. ter Haar, and D. Cranston, "High intensity focused ultrasound: surgery of the future?" Br. J. Radiol. **76**, 590-599 (2003).

12. J. E. Kennedy, F. Wu, G. ter Haar, F. V. Gleeson, R. R. Phillips, M. R. Middleton, and D. Cranston, "High-intensity focused ultrasound for the treatment of liver tumours," Ultrasonics, **42**, 931-935 (2004).

13. S. Madersbacher, M. Pedevilla, L. Vingers, M. Susani, and M. Marberger, "Effect of high-intensity focused ultrasound on human prostate cancer in vivo," Cancer Res. **55**, 3346-3351 (1995).

14. E. A. Stewart, J. Rabinovici, C. M. C. Tempany, Y. Inbar, L. Regan, B. Gastout, G. Hesley, H. S. Kim, S. Hengst, and W. M. Gedroye, "Clinical outcomes of focused ultrasound surgery for the treatment of uterine fibroids," Fertil. Steril. **85**, 22-29 (2006).

15. F. Wu, Z. B. Wang, W. Z. Chen, J. Bai, H. Zhu, and T. Y. Qiao, "Preliminary experience using high intensity focused ultrasound for the treatment of patients with advanced stage renal malignancy," J. Urol. 1**70**, 2237-2240 (2003).

16. F. Wu, Z. B. Wang, W. Z. Chen, J. Z. Zou, J. Bai, H. Zhi, K. Q. Li, F. L. Xie, C. B. Jin, H. B. Su, and G. W. Gao, "Extracorporeal focused ultrasound surgery for treatment of human solid carcinomas: early Chinese clinical experience," Ultrasound Med. Biol. **30**, 245-260 (2004).

17. L. L. Xiong, J. H. Hwang, X. B. Huang, S. S. Yao, C. J. He, X. H. GE, H. Y. Ge, and X. F. Wang, "Early clinical experience using high intensity focused ultra-sound for palliation of inoperable pancreatic cancer," JOP J. Pancreas, **10**, 123-129 (2009).

18. C. C. Wu, C. N. Chen, M. C. Ho, W. S. Chen, and P. H. Lee, "Using the acoustic interference pattern to locate the focus of a high-intensity focused ultrasound (HIFU) transducer," Ultrasound Med. Biol. **34**, 137-146 (2008).

19. X. Zheng and S. Vaezy, "An acoustic backscatter-based method for localization of lesions induced by high-intensity focused ultrasound," Ultrasound Med. Biol. **36**, 610-622 (2010).

20. J. Hindley, W. M. Gedroyc, L. Regan, E. Stewart, C. Tempany, K. Hynnen, N. Macdanold, Y. Inbar, Y. Itzchak, J. Rabinovici, K. Kim, J. F. Geschwind, G. Hesley, B. Gostout, T. Ehrenstein, S. Hengst, M. Sklair-Levy, A. Shushan, and F. Jolesz, "MRI guidance of focused ultrasound therapy of uterine fibroids: Early results," Am. J. Roentgenol. **183**, 1713-1719 (2004).

21. N. McDannold, C. M. Tempany, F. M. Fennessy, M. J. So, F. J. Rybicki, E. A. Stewart, F. A. Jolesz, and K. Hynynen, "Uterine Leiomyomas: MR imaging-based thermometry and thermal dosimetry during focused ultrasound thermal ablation," Radiology, **240**, 263-272 (2006).

22. C. Bohris, W. G. Schreiber, J. Jenne, I. Simiantonakis, R. Rastert, H. J. Zabel, P. Huber, R. Bader, and G. Brix, "Quantitative MR temperature monitoring of high-intensity focused ultrasound therapy," Magn. Reson. Imaging. **17**, 603-610 (1999).

23. E. S. Ebbini, H. Yao, and A. Shrestha, "Dual-mode ultrasound phased arrays for image-guided surgery," Ultrasonic Imaging, **28**, 65-82 (2006).

24. A. Anand, D. Savery, and C. Hall, "Three-dimensional spatial and temporal temperature imaging in gel phan-toms using backscattered ultrasound," IEEE Trans. Ultrason. Ferroelect. Freq. Contr. **54**, 23-31 (2007).

25. P. D. Bevan and M. D. Sherar, "B-scan ultrasound imaging of thermal coagulation in bovine liver: log envelope slope attenuation mapping," Ultrasound Med. Biol. **27**, 379-387 (2001).

26. P. D. Bevan and M. D. Sherar, "B-scan ultrasound imaging of thermal coagulation in bovine liver: fre-quency shift attenuation mapping," Ultrasound Med. Biol. **27**, 809-817 (2001).

27. E. E. Konofagou, J. Thierman, T. Karjalainen, and K. Hynynen, "The temperature dependence of ultrasound-stimulated acoustic emission," Ultrasound Med. Biol. **28**, 331-338 2002).

28. R. Seip and E. S. Ebbini, "Noninvasive estimation of tissue temperature response to heating fields using diagnostic ultrasound," IEEE Trans. Biomed. Eng. **42**, 828-839 (1995).

29. V. A. Khokhlova, S. M. Bobkova, and L. R. Gavrilov,

"Focus splitting associated with propagation of focused ultrasound through the rib cage," Acoust. Phys. **56**, 622-632 (2010).

30. F. Li, X. Gong, K. Hu, C. Li, and Z. Wanng, "Effect of ribs in HIFU beam path on formation of coagulative necrosis in goat liver," Proc. the 5th International Symposium on Therapeutic Ultrasound. Oxford, UK, **829**, 447-480 (2006).
31. C. Lafon, V. Zderic, M. L. Nobel, J. C. Yuen, P. J. Kaczkowski, O. A. Sapozhnikov, F. Chavrier, L. A. Crum, and S. Vaezy, "Gel phantom for use in high-intensity focused ultrasound dosimetry," Ultrasound Med. Biol. **31**, 1383-1389 (2005).
32. B. A. Rabkin, V. Zderic, and S. Vaezy, "Hyperecho in ultrasound images of HIFU therapy: Involvement of cavitation," Ultrasound Med. Biol. **31**, 947-956 (2005).

Profile

▸ Jae Hee Song (송재희)

Jae Hee Song received the B.S. degree in computer science in 2004, the M.S. degree in electronic engineering in 2006, and the Ph.D. degree in an interdisciplinary program of integrated biotechnology in 2012 from Sogang University, Seoul, Korea. From 2012 to 2014, he was a Postdoctoral Researcher at Medical Solutions Institute, Sogang Institutes of Advanced Technology. In 2014, he joined the Cavitation Laboratory at the University of Dundee, UK, relocated to the University of Glasgow, Glasgow, UK. Currently he is a Senior Research Officer with Queensland Brain Institute at University of Queensland, translating focused ultrasound techniques into pre- and clinical applications. His research interests include medical imaging and therapy technologies using ultrasound, more specifically monitoring and control of cavitation as well as fundamental understanding of the physical behaviour of acoustically driven bubbles.

▸ Jin Ho Chang (장진호)

Jin Ho Chang received his B.S. and M.S. degrees in Electronic Engineering from Sogang University, Seoul, Korea, in 2000 and 2002, respectively. He obtained his Ph.D. degree in Biomedical Engineering from the University of Southern California, Los Angeles, CA, in 2007. Currently He is a professor of the Department of Biomedical Engineering and Department of Electronic Engineering, Sogang University, Seoul, Korea. His research interests include photoacoustic imaging and its clinical applications, high-frequency ultrasound imaging systems, therapeutic ultrasound, and biomedical signal processing.

▸ Yangmo Yoo (유양모)

Yangmo Yoo received the B.S. and M.S. degree from the Department of Electronic Engineering from Sogang University, Seoul, Korea, in 1999 and 2001, respectively, and the Ph.D. degree from the Department of Bioengineering from the University of Washington, Seattle, WA, USA, in 2007. From 2007 to 2009, he was a Systems Design Engineer with Philips Healthcare, Bothell, WA. He is currently a Professor of electronic engineering and biomedical engineering, Sogang University. His research interests include medical ultrasound imaging and its clinical applications in diagnostics and therapy.